Trajectory and Attitude Determination of a Thrusting Spin-Stabilized Apogee Stage

V. Adimurthy,* P. V. Subba Raju,† and D. R. Manohar†
Vikram Sarabhai Space Centre, Trivandrum, India

The injection state vector is estimated from the analysis of data from suitable sensors mounted on a thrusting spin-stabilized apogee stage of a launch vehicle. Here, in addition to the velocity increments obtained from an onboard velocity encoder, the attitude variations during the thrusting phase are important. A new method is presented to determine the inertial pitch and yaw attitude variations of the longitudinal axis using only horizon-crossing sensors. This global method takes into account the dynamical coupling of the pitch and yaw motions, and thus avoids the multiple sensor data needed for the cone-intersection methods. The attitude and velocity encoder information is then combined with the initial state vector input from the inertial navigation system at the separation of the previous stage to generate the trajectory history. These operations, which can be performed in near real time from the telemetered sensor data, are tested using a dynamics simulator. It is shown through a Monte Carlo error analysis that the injection point can be estimated with an accuracy sufficient for preliminary orbit determination.

Nomenclature

$\boldsymbol{a}$	= acceleration vector
$\boldsymbol{F}$	= specific force vector
$[\boldsymbol{F}]^B$	= $\boldsymbol{F}$ expressed in body-fixed frame
g	= acceleration due to gravity
I_{xx}	= moment of inertia along longitudinal axis
I_{yy}, I_{zz}	= moments of inertia along lateral axes
$\boldsymbol{l}_1$	= unit vector along longitudinal axis
$\boldsymbol{l}_2, \boldsymbol{l}_3$	= unit vectors along lateral body axes
L	= angle defined in Fig. 1
p, q, r	= components of $\boldsymbol{\omega}$ in body frame
R_θ, I_θ	= real and imaginary parts of digital Fourier transform coefficients of θ
R_ψ, I_ψ	= real and imaginary parts of digital Fourier transform coefficients of ψ
$\boldsymbol{r}$	= position vector from c.g. to point P
$\boldsymbol{V}$	= output of strapdown integrating accelerometers
V_1	= component of $\boldsymbol{V}$ along $\boldsymbol{l}_1$ direction
$\dot{V}_1$	= time derivative of V_1
α	= horizon-crossing sensor mounting angle (Fig. 1)
η	= thrust misalignment azimuthal angle
θ_L	= local pitch attitude angle (Fig. 1)
θ_I	= inertial pitch attitude angle
Θ	= digital Fourier transform of θ data
β	= $(I_{yy} - I_{xx})/I_{zz}$
ϵ	= I_{xx}/I_{zz}
μ	= half-Earth pulse-width angle (Fig. 1)
ζ	= thrust misalignment axial angle
ψ_I	= inertial yaw attitude angle
$\boldsymbol{\omega}$	= angular velocity vector

Subscripts

P	= accelerometer mounting point
CG	= instantaneous center of gravity

Received Nov. 25, 1985; revision received June 2, 1986.

*Head, Aerodynamics Division.
†Scientist, Aerodynamics Division.

Introduction

EARLY orbit determination, soon after the launch phase of a satellite launch vehicle, is often operationally required for a preliminary knowledge of the vehicle performance and for satellite acquisition management from ground stations. Methods based on differential corrections[1] are limited in their applicability as they need a good initial estimate for convergence, because only short-arc information is normally available at injection. Using nonlinear function-minimization techniques, Adimurthy and Joy[2] and Sheela and Bhat[3] have proposed methods to improve the domain of convergence.

In this paper, an alternate approach to estimating the injection state vector is presented through the analysis of data from a set of sensors mounted on the thrusting spin-stabilized apogee stage. Here, in addition to the velocity increment, the attitude variations during the thrusting phase are important. Even though the inertial attitude of a spin-stabilized apogee motor ideally is constant, precessional and nutational motions are generated due to separation disturbances, thrust misalignments, dynamic unbalance, and jet damping. Waterfall,[4] Menon and Sunderarajan,[5] and several others have analytically studied the spinning upper-stage dynamics. Waterfall has also addressed the inaccuracy in the velocity increment vector due to individual causes of attitude variations. However, no attempt has been made to synthesize a near-real-time attitude determination scheme with velocity increments in order to obtain the injection state vector. In this paper, we propose a new approach to global attitude determination for spin-stabilized thrusting bodies using horizon sensors alone which, when coupled with uniaxial velocity encoder outputs, can give the injection state vector to an accuracy sufficient for preliminary orbit determination. This will be part of an experiment[6] on the launch vehicle monitoring payload of the ASLV mission of the Indian Space Research Organisation. In addition to determining the initial estimate of the orbit through the injection state vector, this experiment also aims at evaluating the performance of the final stage of the launch vehicle.

The attitude of a space vehicle is usually determined point-to-point using different combinations of sensors, such as magnetometers, sun sensors, horizon sensors, and star sensors. When magnetometers are used for attitude determination, in-flight estimation of biases is often necessary,[7] apart from taking into account uncertainties and fluctuations in the magnetic-field model. Unmodeled bias errors in sun sensors and

magnetometers can cause divergence in sequential estimation techniques.[8] Even though star sensors are successfully used for attitude determination of spinning vehicles in various satellite missions,[9] they are expensive and their computer software requirements are high. With horizon sensors, operational accuracies better than 0.1 arc deg can be achieved for low-altitude Earth orbits.[10,11]

In the present experiment on the ASLV mission, in addition to a velocity encoder strapped along the longitudinal axis of the stage, three types of attitude sensors are available on-board. They are 1) two infrared horizon-crossing sensors (mounted at 45 and 135 deg to the longitudinal spin axis) with a 3-sigma accuracy of 0.06 deg in Earth aspect angle, 2) a twin-slit sun sensor with an accuracy of 0.5 deg in sun aspect angle, and 3) a triaxial magnetometer with a total angular error of 0.75 deg. The stage itself is spin-stabilized with a nominal 135 rotations/min spin rate, burns for 35 s, and places the satellite into a nearly circular orbit of 400-km altitude. Since there is a large difference between the accuracy of the horizon sensors and that of the other available sensors, attitude determination based on cone-intersection methods deteriorates the overall accuracy. This situation motivates us to search for methods using single types of sensors alone to obtain the inertial pitch and yaw attitudes of the longitudinal axis.

Single-axis attitude determination methods for spinning spacecraft are described by Wertz in Ref. 12. These can be classified as deterministic estimators based on cone-intersection techniques and as optimal batch estimators by block averaging. Shuster[13] improves these algorithms by reducing the dependence on solution of trigonometric equations. In the cone-intersection approaches, multiple sensor data at a given instant of time are required. In batch estimation of the spin axis, it is assumed that the orientation can be considered fixed over a period of time. While this is a valid assumption under normal spacecraft conditions, attitude variations are important during the thrusting period of a spin-stabilized apogee motor.

The global attitude determination scheme presented in this paper takes into account the dynamics of coning motion. From the horizon-crossing sensor output, one can directly obtain the angle betwen spin axis and the local horizontal plane. This angle is termed as local pitch angle in this paper. It is shown that the inertial pitch-angle variations can be estimated from local pitch angle by removing the low-frequency components due to translational motion. The yaw angle variations are then obtained from the pattern of dynamical coupling of the pitch and yaw attitude motions. This coupling can be stated in terms of the coefficients of the digital Fourier transforms. The inertial attitude variations thus obtained are added to the initial attitude known from the inertial navigation system of the previous stage, which is separated after the apogee stage is spun over a spin bearing. This attitude information is then coupled with the data of a single-axis velocity encoder mounted along the longitudinal axis of the vehicle and is integrated to generate the injection state vector. The methodology and justification of this scheme are described in detail. A near-real-time software for these operations is developed. This software is tested under various dynamical conditions applicable to thrusting spin-stabilized apogee motors. A Monte Carlo error analysis shows that the injection point can be estimated with an accuracy sufficient for preliminary orbit determination.

Basic Methodology

In the present configuration, the apogee motor is first spun over a spin bearing, and then the previous unspun stage, carrying a stabilized platform inertial navigation system, is separated. The INS output at the separation instant will provide the initial state vector for further analysis of apogee motor dynamics. For a spin-stabilized apogee motor, a single-axis integrating accelerometer aligned along the longitudinal spin axis is a sufficient sensor for the requirement of velocity increments. If strapdown accelerometers along the lateral axes are provided, their outputs will be dominated by contributions due to rotation of the vehicle through dynamic unbalance, sensor offsets, and misalignments rather than to external forces. Studies presented later in this paper confirm that the actual effect of dispensing with lateral accelerometers is small.

The acceleration equation with a single integrating accelerometer strapped down along the longitudinal axis will now be derived. The output V of an integrating accelerometer is $\int [\boldsymbol{F}]^B \mathrm{d}t$, where $\boldsymbol{F}$ is the specific force, which is the difference between the inertial acceleration at point P, where the accelerometer is mounted, and the gravitational acceleration.[14]

$$\boldsymbol{F}_P = \boldsymbol{a}_p - \boldsymbol{g} \tag{1}$$

The acceleration at point P is related to the acceleration at center of gravity CG by

$$\boldsymbol{a}_P = \boldsymbol{a}_{\mathrm{CG}} + \boldsymbol{\omega} \times (\boldsymbol{\omega} \times \boldsymbol{r}) + \dot{\boldsymbol{\omega}} \times \boldsymbol{r} \tag{2}$$

Assuming that terms proportional to the rate of change of $\boldsymbol{\omega}$ are small,

$$\boldsymbol{a}_P = \boldsymbol{a}_{\mathrm{CG}} + \boldsymbol{\omega} \times (\boldsymbol{\omega} \times \boldsymbol{r})$$

Hence,

$$\boldsymbol{a}_{\mathrm{CG}} = \boldsymbol{F}_p + \boldsymbol{g} - \boldsymbol{\omega} \times (\boldsymbol{\omega} \times \boldsymbol{r}) \tag{3}$$

Assuming that the acceleration due to gravity is the same at CG and point P,

$$\boldsymbol{F}_P = \boldsymbol{F}_{\mathrm{CG}} + \boldsymbol{\omega} \times (\boldsymbol{\omega} \times \boldsymbol{r}) \tag{4}$$

The specific force $\boldsymbol{F}_P$ at P can have substantial components along the lateral directions due to sensor offsets, misalignments, etc. $\boldsymbol{F}_{\mathrm{CG}}$, however, can be assumed to be along the longitudinal direction $\boldsymbol{l}_1$ for the purpose of force equation integration in view of $p \gg q, r$. This implies that

$$\boldsymbol{F}_{\mathrm{CG}} \cdot \boldsymbol{l}_2 = 0, \qquad \boldsymbol{F}_{\mathrm{CG}} \cdot \boldsymbol{l}_3 = 0 \tag{5}$$

Hence, the components of $\boldsymbol{F}_P$ along the $\boldsymbol{l}_1$, $\boldsymbol{l}_2$, and $\boldsymbol{l}_3$ directions can be written as

$$\boldsymbol{F}_P \cdot \boldsymbol{l}_i = \boldsymbol{F}_{\mathrm{CG}} \cdot \boldsymbol{l}_1 + [\boldsymbol{\omega} \times (\boldsymbol{\omega} \times \boldsymbol{r})] \cdot \boldsymbol{l}_1 \tag{6a}$$

$$\boldsymbol{F}_P \cdot \boldsymbol{l}_2 = [\boldsymbol{\omega} \times (\boldsymbol{\omega} \times \boldsymbol{r})] \cdot \boldsymbol{l}_2 \tag{6b}$$

$$\boldsymbol{F}_P \cdot \boldsymbol{l}_3 = [\boldsymbol{\omega} \times (\boldsymbol{\omega} \times \boldsymbol{r})] \cdot \boldsymbol{l}_3 \tag{6c}$$

Substituting Eqs. (6) in Eq. (3),

$$\boldsymbol{a}_{\mathrm{CG}} = \boldsymbol{g} + (\boldsymbol{F}_P \cdot \boldsymbol{l}_1)\boldsymbol{l}_1 - \{[\boldsymbol{\omega} \times (\boldsymbol{\omega} \times \boldsymbol{r})] \cdot \boldsymbol{l}_1\}\boldsymbol{l}_1 \tag{7}$$

Since

$$V = \int [\boldsymbol{F}_P]^B \mathrm{d}t, \quad V_1 = \int (\boldsymbol{F}_P \cdot \boldsymbol{l}_1) \mathrm{d}t, \quad \dot{V}_1 = \boldsymbol{F}_P \cdot \boldsymbol{l}_1 \tag{8}$$

we obtain the final acceleration equation

$$\boldsymbol{a}_{\mathrm{CG}} = \boldsymbol{g} + \dot{V}_1 \boldsymbol{l}_1 - \{[\boldsymbol{\omega} \times (\boldsymbol{\omega} \times \boldsymbol{r})] \cdot \boldsymbol{l}_1\}\boldsymbol{l}_1 \tag{9}$$

With the knowledge of the time history of $\boldsymbol{l}_1$, Eq. (9) can be integrated to obtain the state vector history.

The method of generating the inertial attitude variations of the longitudinal axis $\boldsymbol{l}_1$ of the spinning apogee motor is described in the next section.

Global Attitude Determination

The method of spin-axis attitude determination described in this paper is termed global attitude determination in contrast to point-to-point attitude determination by cone-intersection methods, batch determination by the least-squares approach, or sequential estimation by the Kalman filter technique. As outlined in the Introduction, the data from horizon-crossing sensors over a period of time are analyzed in the frequency domain. The low-frequency variations due to changes in the local vertical are removed, and the dynamical coupling between pitch and yaw angles is utilized to obtain the yaw angle variations from the inertial pitch-angle variations. (Here the inertial yaw angle ψ_I is defined as the angle between l_1 and the fixed reference plane, defined at the instant of apogee motor ignition by l_1 and the local vertical. Similarly, the inertial pitch angle θ_I is the angle between the projection of l_1 onto the reference plane defined above and a fixed line in the reference plane.) Thus, the present method enables determination of attitude variations of a spinning body from a single class of onboard sensors.

Determination of Inertial Pitch Angle

The horizon-crossing sensors measure the angle between the vehicle spin axis and the local horizontal plane in terms of Earth pulse widths.

The measurement geometry of a single horizon sensor is shown in Fig. 1. As shown by Fang[15]

$$\cos L = -\sin\theta_L \cos\alpha + \cos\theta_L \sin\alpha \cos\mu \tag{10}$$

When two horizon-crossing sensors, with mounting angles α_1 and α_2, measure the Earth pulse widths $2\mu_1$ and $2\mu_2$, respectively, then $\cos L$ can be eliminated to give the expression for local pitch angle as

$$\tan\theta_L = \frac{\sin\alpha_1 \cos\mu_1 - \sin\alpha_2 \cos\mu_2}{\cos\alpha_1 - \cos\alpha_2} \tag{11}$$

The local pitch attitude angle history consists of variations due to coning, nutation, and local vertical variation. A typical example of the variation of local pitch attitude angle is shown in Fig. 2. This is generated using a six-degrees-of-freedom vehicle dynamics simulator.[16] The frequency spectrum corresponding to data in Fig. 2 is given in Fig. 3. On the other hand, the temporal variation of the inertial pitch angle θ_I and its frequency spectrum are given in Figs. 4 and 5, respectively. The difference between the variation of θ_I and θ_L is due mainly to the change in local vertical direction. This occurs as a result of the translational motion of the apogee motor during the course of its burning and is limited to a few degrees. This is reflected in the frequency domain as additional low-frequency components in θ_L. Thus, one way to obtain θ_I variations from θ_L variations is to clip the low-frequency portion and retain the easily identifiable frequencies of coning and nutation. To minimize the error due to this transformation, the low-frequency components are not totally removed but are smoothly interpolated to zero.

Digital Fourier transforms (DFT) are used to determine the frequency content of the local pitch attitude angle θ_L, using standard library subroutines of fast Fourier transform (FFT). It may be recalled that the sequence of N data points of the pitch angle $\theta(k)$, $k=1,2,\ldots,N$ is related to the sine-cosine coefficients of the DFT by

$$\theta(k) = \frac{1}{N}\sum_{n=0}^{N-1}[R_\theta(n) + iI_\theta(n)]\exp(i2\pi nk/N)$$
$$= \frac{1}{N}\sum_{n=0}^{N-1}\Theta(n)\exp(i2\pi nk/N) \tag{12}$$

where $\Theta(n)$ is the DFT of $\theta(k)$ given by

$$\Theta(n) = \sum_{k=0}^{N-1}\theta(k)\exp(-i2\pi nk/N) \tag{13}$$

Determination of Inertial Yaw Angle

It may be impossible to determine the inertial pitch and yaw attitude angles geometrically from the local pitch angle alone at any given instant. However, it is possible in a global sense because of the systematic behavior of a spin-stabilized apogee motor, resulting in a dynamical coupling between pitch and yaw motions. For example, if jet damping is neglected, it has been shown by Kolk,[17] under assumptions fairly valid for spin-stabilized rockets, that

$$\theta = L_1 \sin p_0\epsilon t - L_2(1-\cos p_0\epsilon t) + L_3 \sin p_0\beta t - L_4(1-\cos p_0\beta t) \tag{14}$$

$$\psi = L_1(1-\cos p_0\epsilon t) + L_2 \sin p_0\epsilon t + L_3(1-\cos p_0\beta t) + L_4 \sin p_0\beta t \tag{15}$$

where L_1, L_2, L_3, and L_4 depend on the initial attitude rate disturbances, initial spin rate p_0, thrust misalignment, and the dynamic unbalance.

Considering the effect of jet damping, it has been observed[4,5,17] that the terms with coefficients L_1 and L_2 are

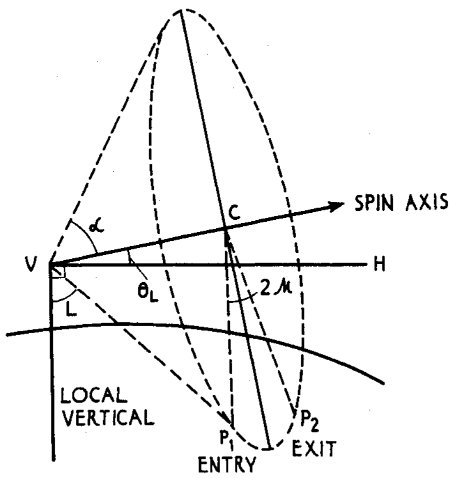

Fig. 1 Geometry of horizon-crossing sensor measurement.

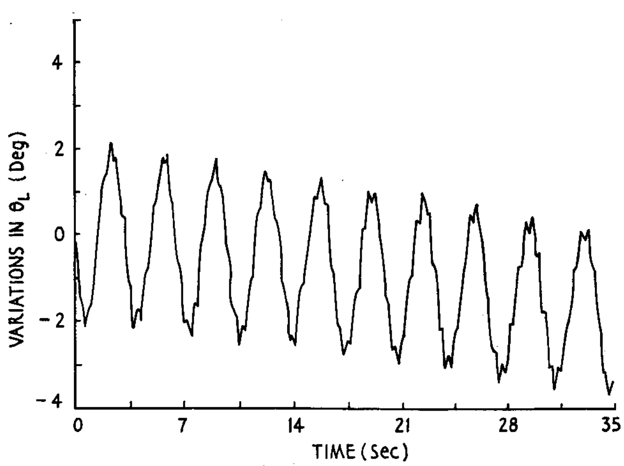

Fig. 2 Variations of local pitch angle.

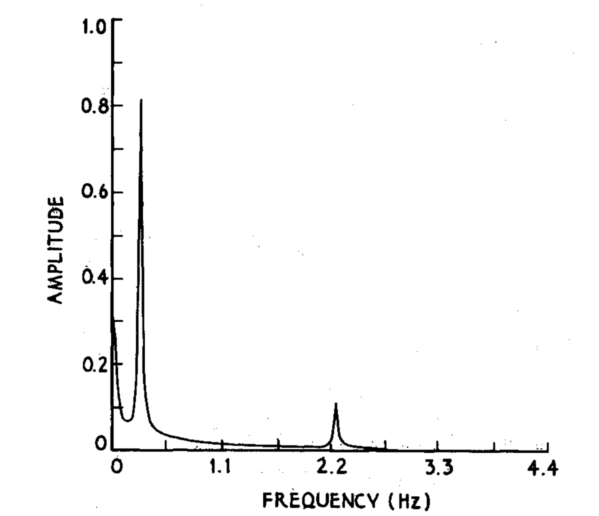

Fig. 3 Frequency spectrum of local pitch angle.

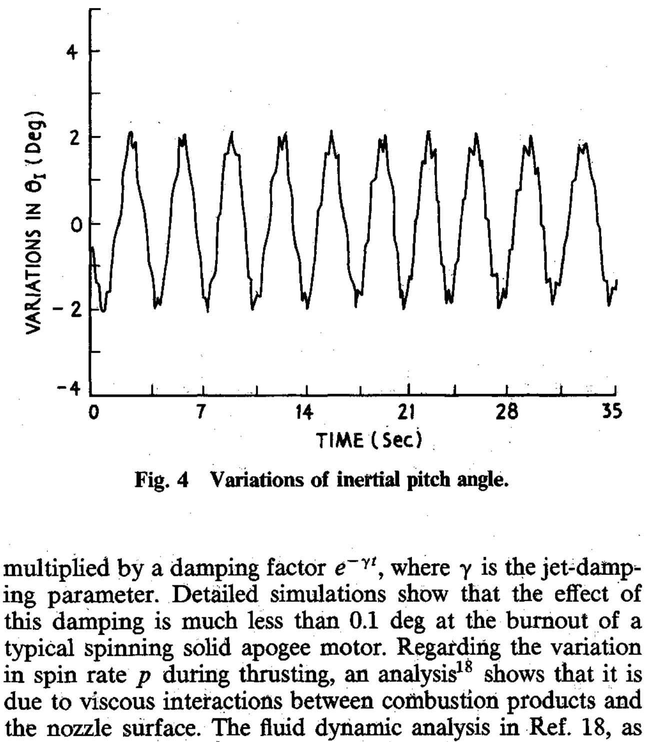

Fig. 4 Variations of inertial pitch angle.

multiplied by a damping factor $e^{-\gamma t}$, where γ is the jet-damping parameter. Detailed simulations show that the effect of this damping is much less than 0.1 deg at the burnout of a typical spinning solid apogee motor. Regarding the variation in spin rate p during thrusting, an analysis[18] shows that it is due to viscous interactions between combustion products and the nozzle surface. The fluid dynamic analysis in Ref. 18, as well as actual flight experiences, shows that the variation in p is small. Hence, the cross-coupling variations in pitch and yaw angles due to variations in spin rate can be assumed small.

Based on these considerations, it is proposed in this paper that the systematic coupling between the general variations in inertial pitch and yaw angles of thrusting spin-stabilized apogee motor can be quantified in terms of the sine and cosine coefficients in frequency domain in the following form:

$$R_\theta(n) = \pm I_\psi(n) \tag{16}$$

$$I_\theta(n) = \mp R_\psi(n) \tag{17}$$

The sign depends on the sense of initial spin rate p_0.

Equations (16) and (17) allow one to estimate the inertial yaw angle variations from known variations of inertial pitch angle. These variations are then added to the initial attitude from the navigation system at the ignition of the apogee motor.

This methodology of attitude estimation is applied to a typical simulated case. Figure 6 shows the comparison between the estimated inertial pitch angle and the actual simulated pitch angle. Similarly, Fig. 7 shows the estimated and actual yaw angles. These comparisons show that the dynamical variations in pitch and yaw are fairly well estimated, indicating this method as a good candidate for attitude determination leading to injection state vector estimation.

Injection State Vector Estimation

A computer program is developed to integrate the acceleration equation (9), using the approach of the previous section to obtain l_1, the instantaneous attitude of the longitudinal axis. Keeping in view the need of early orbit determination, this program is configured on a ground computer in a near-real-time mode. A functional diagram of this software, named Velocity Increment Determination Experiment Near Real Time (VIDE NRT) program,[19] is given in Fig. 8. The data from the single-axis integrating accelerometer and the Earth entry and exit times from the two horizon-crossing sensors are received through telemetry channels. These are edited and smoothed according to standard procedures. The data are then compensated for known bias and nonlinearity errors. The components of acceleration due to gravity take into account oblateness of Earth up to J_2. These are computed in an Earth-centered inertial (ECI) system, which is also the basic integration frame. For the fast Fourier transforms and their inverses, used in the determination of θ and ψ, standard routines available on the International Mathematical and Statistical Library (IMSL) are used. After the thrust phase is over, the orbital elements are calculated from the injection state vector. Complete details of the software are given in Ref. 19.

Test Plan and Results

In order to test the VIDE NRT software under various operating conditions, a dynamics simulator is required, both for input generation and output evaluation. A six-degrees-of-freedom launch-vehicle simulation program, COMETS,[16] is used for this purpose. This is the standard package for trajectory simulation and software test activities for launch vehicles at Vikram Sarabhai Space Centre and has been sufficiently validated. In the present situation, the spacecraft is still in the launch phase, with none of its onboard control systems as yet active and none of its solar panels deployed; therefore, a six-degrees-of-freedom simulation is sufficient. However, for the present test plan, COMETS has been augmented to simulate the sensor position and alignment errors using quaternion transformations. Sensor dynamical errors are also modeled.

In the test plan presented in Table 1, a number of COMETS simulation runs are made to generate input files corresponding to five dynamical conditions of the apogee stage, representing different thrust misalignment azimuthal angles, different combinations of initial pitch and yaw disturbance rates, and large underperformance and overperformance of previous stages. A nominal dynamic unbalance of 0.2 deg is considered in all cases.

Table 1 Test plan for VIDE NRT software

Case no.	Thrust misalignment deg, ζ/η	Initial rates, deg/s, q/r	Initial state vector
1	0.3/0.0	1.0/0.0	Standard[a]
2	0.3/180.0	1.0/0.0	Standard
3	0.3/0.0	0.0/1.0	Standard
4	0.3/0.0	1.0/0.0	Underperformance[b]
5	0.3/0.0	1.0/0.0	Overperformance[c]

[a]Standard initial state vector at apogee motor ignition is taken corresponding to nominal performance of previous stages. [b]Standard initial position vector but initial velocity less by 150 m/s in maximum geocentric velocity component. [c]Standard initial position vector but initial velocity greater by 150 m/s in maximum geocentric velocity component.

Table 2 Comparison of VIDE NRT test results with 6-D simulation

Case no.	Injection velocity, Km/s VIDE NRT/6-D	Flight path angle, deg VIDE NRT/6-D	Inclination, deg VIDE NRT/6-D	Apogee altitude, Km VIDE NRT/6-D	Perigee altitude, Km VIDE NRT/6-D
1	7.6635/7.6632	90.025/89.999	46.111/46.078	400.504/400.478	382.944/382.606
2	7.6639/7.6635	90.015/89.995	46.102/46.070	400.659/400.501	384.630/383.545
3	7.6625/7.6618	90.172/90.165	45.947/45.905	412.464/411.104	366.503/365.498
4	7.5617/7.5598	90.102/90.069	46.923/46.890	400.652/400.508	35.478/29.190
5	7.7702/7.7682	89.952/89.928	45.332/45.289	773.789/766.384	400.564/400.484

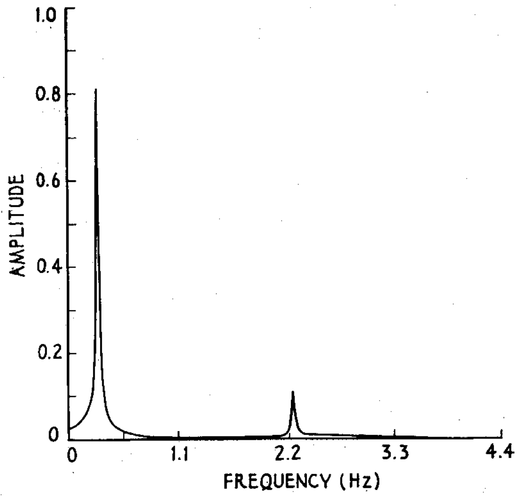

Fig. 5 Frequency spectrum of inertial pitch angle.

Table 3 System error levels

Parameter	Unit	One-sigma error
Initial state vector (INS)		
X, Y, Z	m	150, 500, 200
U, V, W	m/s	1.0, 7.0, 2.0
θ, ψ	deg	0.087, 0.1
Velocity encoder		
Random noise	m/s	0.033
Accelerometer location		
(x, y, z)	m	0.008
Bias	m/s^2	0.001
Nonlinearity	s^2/m	0.2×10^{-5}
Scale factor	—	0.0001
Horizon sensor		
Random noise	deg	0.02
Mounting angles	deg	0.033
Bias	deg	0.033

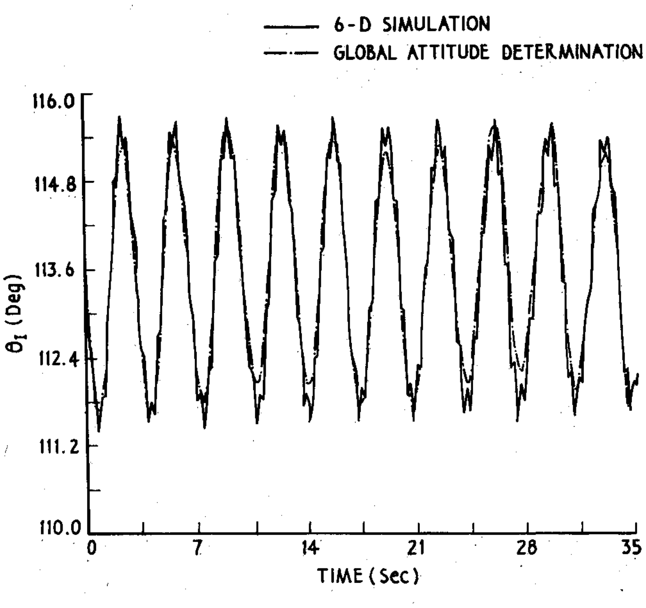

Fig. 6 Estimation of inertial pitch angle.

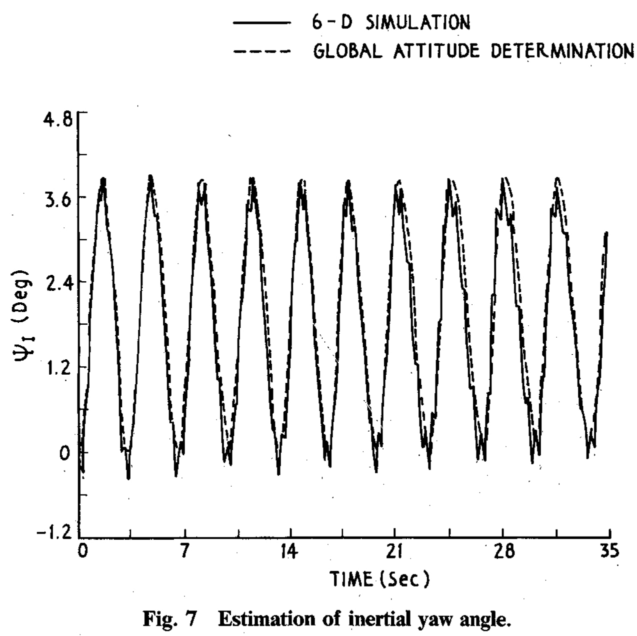

Fig. 7 Estimation of inertial yaw angle.

For the test cases defined in Table 1, the VIDE NRT program is run and the results are given in Table 2. For an integration step size of 0.02 s, each run takes approximately 15 cps for execution on the CDC Cyber 170/730 system at VSSC. In all cases studied, the error in injection velocity is less than 2.0 m/s. The maximum error occurs for the cases of gross over- or underperformance. In other cases, the velocity error is much less than 1.0 m/s. These errors confirm the adequacy of a single-axis accelerometer for the present experiment. The errors in flight path angle and orbital inclination are less than 0.05 deg. The apogee and perigee altitudes are also shown in Table 2. The differences here are mostly less than 5 km, except in cases of over- or underperformance, where they can reach 7 km. This study shows that the new methodology of VIDE NRT program is valid under all the dynamical conditions considered.

Monte Carlo Error Analysis

A detailed Monte Carlo error analysis is done to evaluate the accuracy of the present software under specified sensor and system uncertainties. The parameters considered and their error levels are given in Table 3. During 35-s burn time of the

Table 4 Estimation accuracies of injection state vector

Parameter	Unit	One-sigma accuracy
Velocity	m/s	1.36
Flight path angle	deg	0.036
Azimuth	deg	0.062
Altitude	m	227.0
Latitude	deg	0.0034
Longitude	deg	0.0036
Pitch angle	deg	0.106
Yaw angle	deg	0.104

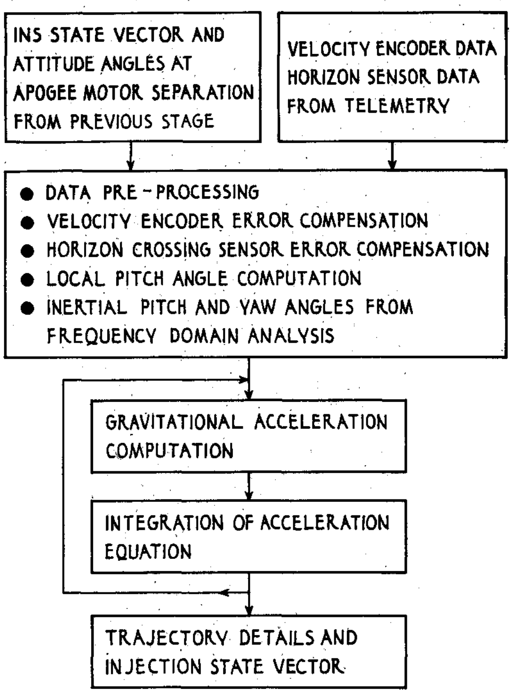

Fig. 8 Functional diagram of VIDE NRT software.

apogee motor, 240 velocity encoder values and 80 sets of transit times for each horizon-crossing sensor will be available. These and all the other parameters given in the table are corrupted by error values generated through an IMSL random number generator. After generating one complete set, the VIDE NRT software is executed and the injection state vector stored. This is sequentially repeated many times and the ensemble of injection state vectors statistically analyzed. The results after 1000 executions of the software are given in Table 4. The sufficiency of the number of Monte Carlo experiments is ascertained by comparing the statistics after 500 and 750 executions.

Table 4 shows that the velocity accuracy is much better than the 3 m/s (1 sigma) specified for preliminary orbit determination for this mission.[20] The attitude errors by this method are limited to 0.1 deg, while the corresponding accuracy by standard cone-intersection methods is at best 0.2 deg or more, depending on the combination of sensors.[11]

Conclusions

A new method of global attitude determination is presented for thrusting spin-stabilized apogee stages. Taking into account the dynamical coupling between the pitch and yaw motions, this attitude determination is achieved from the data of horizon-crossing sensors alone. This approach, integrated with the data from a single-axis accelerometer mounted along the longitudinal axis and with INS information at the separation of the previous stage, enables one to determine the injection state vector. A Monte Carlo error analysis and detailed test results show that the present approach gives attitude determination accuracies much better than those obtained by cone-intersection methods and meets the requirements of preliminary orbit determination.

Acknowledgments

The contributions of P. Vilasini and Radhika B. Ramnath in programming and validating COMETS simulator and VIDE NRT computer programs are gratefully acknowledged.

References

[1]Hunt, W.E. and Nayfeh, A.H., "A Nonlinear Correction Method for Orbit Determination," *AIAA Journal*, Vol. 5, June 1967, pp. 1183–1185.

[2]Adimurthy, V. and Joy, K.V., "Extension of Region of Convergence in Orbit Determination Using Function-Minimization Techniques," *Journal of Guidance and Control*, Vol. 1, Nov.–Dec. 1978, pp. 445–446.

[3]Sheela, B.V. and Bhat, R.S., "Preliminary Orbit Determination by a Composite Multivariate Search Strategy," *Journal of Guidance, Control, and Dynamics*, Vol. 8, May–June, 1985, pp. 391–396.

[4]Waterfall, A.P., "The Accuracy of the Velocity Increment Vector of the Black Arrow Third Stage," *Journal of the British Interplanetary Society*, Vol. 22, Aug. 1969, pp. 233–250.

[5]Menon, K.A.P. and Sunderarajan, N., "Analytical Study of Spinning Solid Upper Stage Dynamics," *Journal of the Aeronautical Society of India*, Vol. 32, Feb.–Nov. 1980, pp. 65–76.

[6]Dev, M.S.R., (ed.), "Technological Mission for ASLV-E1," Vikram Sarabhai Space Centre, Trivandrum, India, VSSC-ASLV-MR-29-83, Feb. 1983.

[7]Thompson, R.H., Neal, G.F., and Shuster, M.D., "Magnetometer Bias Determination and Spin-Axis Attitude Estimation for the AMPTE Mission," *Journal of Guidance, Control, and Dynamics*, Vol. 7, July–Aug. 1984, pp. 505–507.

[8]Bhat, R.S. et al., "Orbit and Attitude Determination for Bhaskara," *Proceedings of the International Symposium on Spacecraft Flight Dynamics*, European Space Agency, ESA SP-160, Aug. 1981, pp. 325–332.

[9]Makinson, D.L., Gutshall, R.L., and Volpe, F., "Star Scanner Attitude Determination for OSO-7 Spacecraft," *Journal of Spacecraft and Rockets*, Vol. 10, April 1973, pp. 262–267.

[10]Serradeil, R., De Dianous, A., and Hebert, M., "New Generation of Infrared Horizon Scanning Sensors for Low Altitude Spacecraft," *Acta Astronautica*, Vol. 12, Feb. 1985, pp. 101–106.

[11]Kalakrishnan, B., Narayanaswamy, and Cyriac, M.J., "Launch Phase Attitude Determination Payload for SROSS-I," ISRO Satellite Centre, Bangalore, India, TR-400-(02) (0), Oct. 1983.

[12]Wertz, J.R. (ed.), *Spacecraft Attitude Determination and Control*, D. Reidel, Dordrecht, The Netherlands, 1978, Chaps. 10 and 11.

[13]Shuster, M.D., "Efficient Algorithms for Spin-Axis Attitude Estimation," *Journal of the Astronautical Sciences*, Vol. XXXI, April–June 1983, pp. 237–249.

[14]Miller, R.B., "Strapdown Inertial Navigation Systems: An Algorithm for Attitude and Navigation Computations," Aeronautical Research Laboratories, Melbourne, Australia, ARL-SYS-Rept. 23, Oct. 1980.

[15]Fang, B.T., "Geometric Theory of Horizon Scanners," *Journal of Spacecraft and Rockets*, Vol. 12, Dec. 1975, pp. 776–778.

[16]Ganeshan, A.S., Sarma, T.A.N., and Vilasini, P., "Trajectory Simulation Program for Multi-Engine Configuration Launch Vehicles," Vikram Sarabhai Space Centre, Trivandrum, India, VSSC-TR-13-181-80, Feb. 1980.

[17]Kolk, W.R., *Modern Flight Dynamics*, Prentice-Hall, Englewood Cliffs, NJ, 1961, pp. 229–235.

[18]Adimurthy, V. et al., "Prediction of Spin-Rate History of SLV-3 Fourth Stage," Vikram Sarabhai Space Centre, Trivandrum, India, SLV-SRTT-1-09-78, Sept. 1978.

[19]Radhika, B.R., Vilasini, P., Manohar, D.R., Subbaraju, P.V., and Adimurthy, V., "Software for Velocity Increment Determination Experiment on ASLV-SROSS-1 Mission," Vikram Sarabhai Space Centre, Trivandrum, India, VSSC-ADDG-ARD-001, June 1985.

[20]Raju, S., "Preliminary Orbit Determination Requirements for ASLV Missions," *Proceedings of Workshop-cum-Seminar on Preliminary Orbit Determination*, Indian Institute of Science, Bangalore, India, Jan. 1985, pp. 1–7.